Consistent Finite-Element Response Sensitivity Analysis

J. P. Conte, M.ASCE[1]; P. K. Vijalapura[2]; and M. Meghella[3]

Abstract: This paper examines the important issue of response sensitivities of dynamic models of structural systems to both material and (discrete) loading parameters. Plasticity-based finite-element models of structural systems subjected to base excitation such as earthquake loading are considered. The two methods for computing the response sensitivities, namely, (1) discretizing in time the time continuous-spatially discrete response equations and differentiating the resulting time discrete-spatially discrete response equations with respect to sensitivity parameters, and (2) differentiating the time continuous-spatially discrete response equations with respect to sensitivity parameters and discretizing in time the resulting time continuous-spatially discrete response sensitivity equations, are clearly distinguished. The discontinuities in time of the response sensitivities arising due to material state transitions in the plasticity models, and their propagation from the quadrature point level to the global structural response level are discussed using a specific one-dimensional plasticity model. The procedure to obtain the exact sensitivities of the numerical nonlinear finite-element response, including proper capture of their discontinuities, is formalized. Application examples illustrating the concepts are presented at the end.

DOI: 10.1061/(ASCE)0733-9399(2003)129:12(1380)

CE Database subject headings: Finite element method; Sensitivity analysis; Reliability analysis; Earthquakes; Structural reliability; Plasticity.

Introduction

In seismic reliability analysis of civil structures, the inherent random variability and/or uncertainty associated with both the structure and earthquake dynamic loading must be taken into consideration. Furthermore, in order to evaluate the probability of structural failure or collapse, which occurs in domains of grossly nonlinear response behavior both materially and geometrically, nonlinear finite-element models of structures able to capture the salient features of the actual ultimate structural behavior under strong earthquake shaking are needed. A key ingredient of structural reliability methods is the sensitivities to both system and loading parameters of the structural response/demand quantities used in formulating the limit-state or performance functions defining the various physical limit-states under consideration (Ditlevsen and Madsen 1996). Mathematically, the sensitivity of a vector-based generic response quantity $\mathbf{r}(t)$ with respect to a scalar material or loading sensitivity parameter θ is defined as the partial derivative of $\mathbf{r}(t)$ with respect to θ. Beside their use in structural reliability analysis, finite-element response sensitivities represent an essential ingredient for gradient-based optimization methods needed in structural optimization, structural identification, finite-element model updating, structural health monitoring, and even structural control (in the context of semiactive control systems based on real-time modification of structural system parameters).

This paper focuses on the important issue of computing, using consistent linearization, the exact sensitivities to both structural and loading parameters of any computed response quantity (local or global, kinematic or static) of a plasticity-based nonlinear finite-element structural model. Focus is placed on materially nonlinear-only finite-element analysis, even though the consistent finite-element response sensitivity analysis method discussed herein is general and can be extended to the case of nonlinear geometry without any conceptual difficulties. The material models considered here are based on rate independent classical plasticity theory (i.e., definition of a yield surface within which the material is supposed to be linear elastic) in contrast with generalized plasticity theory (Lubliner 1990-Chapter 3, Miller 1987) which does not require the definition of a yield surface and according to which inelastic deformations/strains start developing from the start of loading. The methodology presented in this paper assumes spatial discretization, using the finite-element method, of the spatio-temporal governing response equations. The resulting ordinary differential equations in time are integrated using a suitable time stepping scheme. The present methodology assumes a displacement-based finite-element formulation and a general-purpose nonlinear analysis finite-element program based on the direct stiffness method.

Two fundamental approaches to compute the response sensitivities of such spatially discretized inelastic dynamic systems are described and compared. The first approach consists of directly differentiating, with respect to the sensitivity parameter θ in question, the semi-discretized (time continuous-spatially discrete) equations of motion governing the dynamic response of the system to yield the differential response sensitivity equations, and then integrating the latter numerically using a time-stepping algorithm. The second approach consists of integrating numerically,

[1]Associate Professor, Dept. of Structural Engineering, 9500 Gilman Drive, Univ. of California at San Diego, La Jolla, CA 92093-0085. E-mail: jpconte@ucsd.edu

[2]Graduate Student, Univ. of California at Berkeley, Berkeley, CA 94720. E-mail: prashant@ce.berkeley.edu

[3]CESI Spa, Via Rubattino, 54, I20134 Milano, Italy. E-mail: meghella@cesi.it

Note. Associate Editor: Gerhart I. Schueller. Discussion open until May 1, 2004. Separate discussions must be submitted for individual papers. To extend the closing date by one month, a written request must be filed with the ASCE Managing Editor. The manuscript for this paper was submitted for review and possible publication on March 12, 2002; approved on May 28, 2003. This paper is part of the ***Journal of Engineering Mechanics***, Vol. 129, No. 12, December 1, 2003. ©ASCE, ISSN 0733-9399/2003/12-1380–1393/$18.00.

using a time-stepping scheme, the semi-discretized equations of motion to yield a set of nonlinear algebraic equations to be solved using a Newton-Raphson iterative scheme, and then differentiating exactly, with respect to the sensitivity parameter θ, the time discrete-spatially discrete response equations to obtain a linear algebraic sensitivity equation once the response is known. Using the two approaches defined above under the general title of *direct differentiation method* (DDM), previous researchers (Choi and Santos 1987; Arora and Cardoso 1989; Tsay and Arora 1990; Zhang and Der Kiureghian 1993; Kleiber et al. 1997) have developed finite-element response sensitivity analysis methods. However, these references do not carefully distinguish between these two approaches. This paper examines the distinction between the two approaches and states the conditions under which they are equivalent. Herein, we refer to the second approach or Method II as the *consistent DDM* in order to highlight this distinction.

Significant research has been dedicated to the general problem of design sensitivity analysis for path dependent problems in the structural optimization community (e.g., Choi and Santos 1987; Arora and Cardoso 1989; Tsay and Arora 1990; Tsay et al. 1990). However, much of this work considers constant (i.e., static) loading, sensitivities with respect to shape parameters (and not constitutive material parameters), and idealized/specialized problems not formulated within a general finite-element analysis framework (e.g., Tsay et al. 1990), which differs from the focus of this paper (response sensitivity analysis of general plasticity-based dynamic structural models with respect to material and loading parameters within a general finite-element analysis framework).

Models based on classical plasticity theory result in response sensitivities that are discontinuous in time. This is due to the material state transitions that occur at discrete times. These discontinuities occur in various response quantities at both the quadrature point level and the global structural level during their numerical integration in time. The physical nature of these discontinuities as well as their propagation from the quadrature point to the global level are illustrated through a simple 1-D plasticity model.

The main motivation for examining and understanding the discontinuities in sensitivities comes from reliability analyses for finding ''design points'' such as FORM and SORM (first-order and second-order reliability methods) (Ditlevsen and Madsen 1996), using gradient based optimization techniques. From the experience of the authors, these discontinuities in the sensitivities crucially affect the rate of convergence of the optimization schemes to the design points (Conte and Vijalapura 1998; Vijalapura et al. 1999).

Formulation

After spatial discretization using the finite-element method, the spatio-temporal equation of motion of a materially nonlinear-only structural system is given by the following nonlinear matrix differential equation:

$$\mathbf{M}(\theta)\ddot{\mathbf{u}}(t,\theta)+\mathbf{C}(\theta)\dot{\mathbf{u}}(t,\theta)+\mathbf{R}[\mathbf{u}(t,\theta),\theta]=\mathbf{F}(t,\theta) \tag{1}$$

where t=time; θ=scalar sensitivity parameter (material or loading variable); $\mathbf{u}(t)$=vector of nodal displacements; $\mathbf{C}$=damping matrix; $\mathbf{M}$=mass matrix, $\mathbf{R}(\mathbf{u},t)$=history dependent internal (inelastic) resisting force vector; $\mathbf{F}(t)$=dynamic load vector; and a superposed dot denotes one differentiation with respect to time. In the case of earthquake ground excitation which is the focus of this research, the dynamic load vector takes the form $\mathbf{F}(t)=-\mathbf{M}\mathbf{L}\ddot{u}_g(t)$ in which $\mathbf{L}$ is an influence coefficient vector and $\ddot{u}_g(t)$ denotes the input ground acceleration history (assuming rigid-soil excitation). Without loss of generality, a single component ground excitation is considered. The potential dependence of each term of the equation of motion on the sensitivity parameter θ is shown explicitly in Eq. (1).

Let $r(t)$ denote a generic scalar response quantity such as displacement, acceleration, local or resultant stress, local or resultant strain, or local/global cumulative plastic deformation. By definition, the sensitivity of $r(t)$ with respect to the material or loading parameter θ is mathematically expressed as the partial derivative of $r(t)$ with respect to the variable θ. The response sensitivity is both a function of time t and sensitivity parameter θ which takes a specific value θ_0 during a sensitivity analysis. By definition, $\partial r(t)/\partial\theta\big|_{\theta=\theta_0}$ is continuous in time at $t=t_0$ if and only if

$$\lim_{\Delta t\to 0}\left.\frac{\partial r(t)}{\partial\theta}\right|_{\substack{\theta=\theta_0\\ t=t_0-\Delta t}}=\lim_{\Delta t\to 0}\left.\frac{\partial r(t)}{\partial\theta}\right|_{\substack{\theta=\theta_0\\ t=t_0+\Delta t}}=\left.\frac{\partial r(t)}{\partial\theta}\right|_{\substack{\theta=\theta_0\\ t=t_0}} \tag{2}$$

Algorithms for response sensitivity computation can be formulated in two ways (Methods I and II) as sketched in Fig. 1. The first method (represented by steps A_1 and A_2 in Fig. 1) consists of first obtaining the semi-discretized (time continuous-spatially discrete) differential equations governing the exact response sensitivity (herein, *exact response sensitivity* refers to the exact sensitivity, with respect to the sensitivity parameter θ, of the exact solution of the time continuous-spatially discrete response equations) and then discretizing them in time, using a time-stepping algorithm, to determine a numerical *approximation* of the exact response sensitivity. Conversely, the second method (represented by steps B_1 and B_2 in Fig. 1) consists of first discretizing in time the semi-discretized equations of motion to obtain a numerical estimate of the exact response (herein, *exact response* refers to the exact solution of the time continuous-spatially discrete response equations) and then differentiating exactly the numerical scheme for the response with respect to the sensitivity parameter θ in order to obtain the exact sensitivity of the numerical (finite-element) response. An interesting question is whether the response sensitivities computed from these two schemes are the same. As shown below, the answer to this question is that it depends on the discretization schemes used to determine numerically the response and response sensitivities (Heinkenschloss 1997) and how these numerical schemes handle the discontinuities exhibited by the response sensitivities.

Exact Sensitivity of Numerical Response (Method II)

In this section, the equations for calculating the response quantities for the dynamic case and a brief description of their numerical calculation are provided. Following this, the sensitivity equations are obtained by exactly differentiating, with respect to the sensitivity parameter θ, the numerical scheme for computing the response.

We assume without loss of generality that the equation of motion (1) is integrated numerically in time using the well-known Newmark-β method of structural dynamics (Chopra 2001), i.e.

$$\begin{aligned}\ddot{\mathbf{u}}_{n+1}&=\left(1-\frac{1}{2\beta}\right)\ddot{\mathbf{u}}_n-\frac{1}{\beta(\Delta t)}\dot{\mathbf{u}}_n+\frac{1}{\beta(\Delta t)^2}(\mathbf{u}_{n+1}-\mathbf{u}_n)\\ \dot{\mathbf{u}}_{n+1}&=(\Delta t)\left(1-\frac{\alpha}{2\beta}\right)\ddot{\mathbf{u}}_n+\left(1-\frac{\alpha}{\beta}\right)\dot{\mathbf{u}}_n+\frac{\alpha}{\beta(\Delta t)}(\mathbf{u}_{n+1}-\mathbf{u}_n)\end{aligned} \tag{3}$$

where α and β=parameters controlling the accuracy and stability of the numerical integration algorithm. Special cases of the

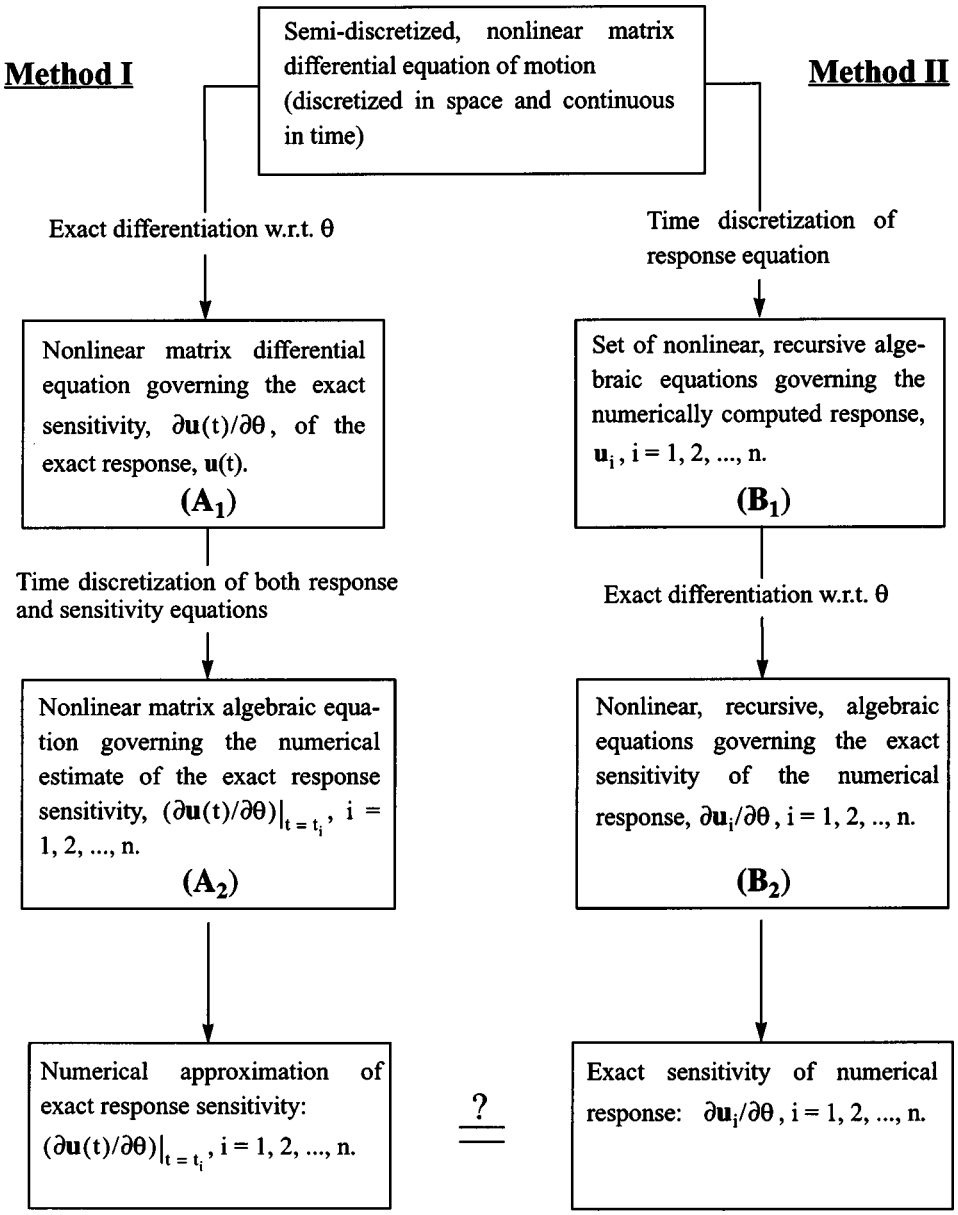

Fig. 1. Flow chart of the two approaches for computing response sensitivities

Newmark-β method are the conditionally stable linear acceleration method ($\alpha=1/2$, $\beta=1/6$) and the unconditionally stable constant average acceleration method ($\alpha=1/2$, $\beta=1/4$). Substitution of Eqs. (3) into equation of motion (1) expressed at discrete time $t=t_{n+1}=(n+1)\,\Delta t$, in which Δt denotes the constant time increment, yields the following nonlinear matrix algebraic equation in the unknowns $\mathbf{u}_{n+1}=\mathbf{u}(t_{n+1})$:

$$\boldsymbol{\Psi}(\mathbf{u}_{n+1})=\tilde{\mathbf{F}}_{n+1}-\left[\frac{1}{\beta(\Delta t)^2}\mathbf{M}\mathbf{u}_{n+1}+\frac{\alpha}{\beta(\Delta t)}\mathbf{C}\mathbf{u}_{n+1}+\mathbf{R}(\mathbf{u}_{n+1})\right]=\mathbf{0} \tag{4}$$

where

$$\tilde{\mathbf{F}}_{n+1}=\mathbf{F}_{n+1}+\mathbf{M}\left[\frac{1}{\beta(\Delta t)^2}\mathbf{u}_n+\frac{1}{\beta(\Delta t)}\dot{\mathbf{u}}_n-\left(1-\frac{1}{2\beta}\right)\ddot{\mathbf{u}}_n\right]+\mathbf{C}\left[\frac{\alpha}{\beta(\Delta t)}\mathbf{u}_n-\left(1-\frac{\alpha}{\beta}\right)\dot{\mathbf{u}}_n-(\Delta t)\left(1-\frac{\alpha}{2\beta}\right)\ddot{\mathbf{u}}_n\right]$$

Eq. (4) represents the set of nonlinear algebraic equations for the unknown response quantities $\mathbf{u}_{n+1}$ that has to be solved at each time step $[t_n, t_{n+1}]$. In the displacement-based finite-element methodology, the vector of internal resisting forces $\mathbf{R}(\mathbf{u}_{n+1})$ in Eq. (4) is obtained by assembling, at the structure level, the vectors of elemental internal resisting forces as

$$\mathbf{R}(\mathbf{u}_{n+1})=\mathop{\mathbf{A}}_{e=1}^{\mathrm{Nel}}\left\{\int_{\Omega_e}\mathbf{B}^T(\mathbf{x})\cdot\boldsymbol{\sigma}[\boldsymbol{\epsilon}_{n+1}(\mathbf{x})]\cdot d\Omega_e\right\} \tag{5}$$

where $\mathbf{A}_{e=1}^{\mathrm{Nel}}\{\ldots\}$ denotes the direct stiffness assembly operator from the element level (in local element coordinates) to the structure level in global reference coordinates; $\mathbf{x}$=vector of spatial coordinates; and $\mathbf{B}$=strain-displacement transformation matrix.

We assume that a Newton-Raphson (or a modified Newton type) iterative procedure is used to solve Eq. (4) over time step $[t_n, t_{n+1}]$ through solving a sequence of linearized problems of the form

$$(\mathbf{K}_T^{\mathrm{dyn}})_{n+1}^{i}\,\delta\mathbf{u}_{n+1}^{i+1}=\boldsymbol{\Psi}_{n+1}^{i} \qquad i=0,1,2,\ldots \tag{6}$$

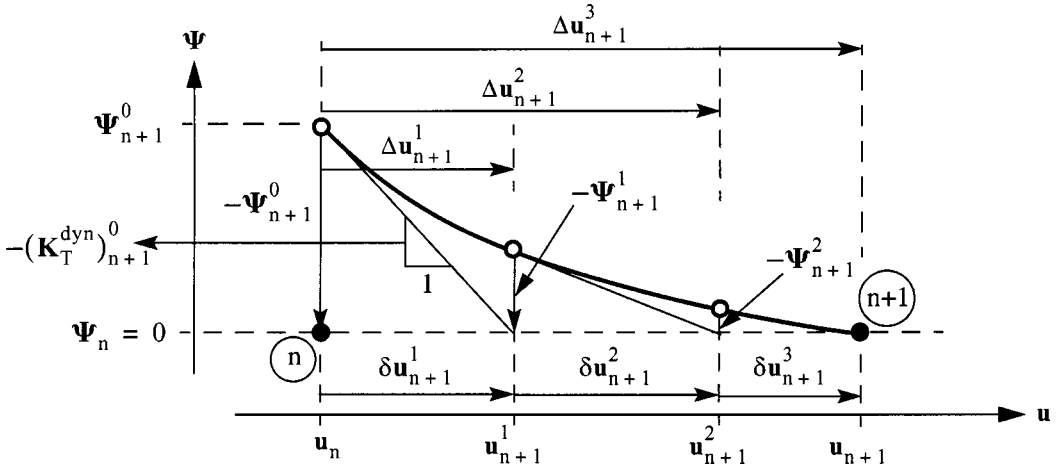

Fig. 2. Graphic representation of iterative Newton-Raphson procedure used to integrate nonlinear equations of motion from time t_n to t_{n+1}

where

$$(\mathbf{K}_T^{\text{dyn}})^i_{n+1} = \left[\frac{1}{\beta(\Delta t)^2}\mathbf{M} + \frac{\alpha}{\beta(\Delta t)}\mathbf{C} + (\mathbf{K}_T^{\text{stat}})^i_{n+1}\right] \tag{7}$$

and

$$\boldsymbol{\Psi}^i_{n+1} = \tilde{\mathbf{F}}_{n+1} - \left[\frac{1}{\beta(\Delta t)^2}\mathbf{M}\mathbf{u}^i_{n+1} + \frac{\alpha}{\beta(\Delta t)}\mathbf{C}\mathbf{u}^i_{n+1} + \mathbf{R}(\mathbf{u}^i_{n+1})\right] \tag{8}$$

The updated nodal displacement vector $\mathbf{u}^{i+1}_{n+1}$, or displacement vector at the end of iteration number $(i+1)$ of time step $[t_n, t_{n+1}]$, is obtained as

$$\mathbf{u}^{i+1}_{n+1} = \mathbf{u}_n + \Delta\mathbf{u}^{i+1}_{n+1} = \mathbf{u}^i_{n+1} + \delta\mathbf{u}^{i+1}_{n+1} \tag{9}$$

where $\Delta\mathbf{u}^{i+1}_{n+1}$ and $\delta\mathbf{u}^{i+1}_{n+1}$ denote the total incremental displacement vector from the last converged step and the last incremental displacement vector, respectively. In Eq. (7), $\mathbf{K}_T^{\text{dyn}}$ denotes the tangent dynamic stiffness matrix and the *consistent or algorithmic (static) tangent stiffness matrix* $(\mathbf{K}_T^{\text{stat}})^i_{n+1}$ in Eq. (7) is obtained as

$$(\mathbf{K}_T^{\text{stat}})^i_{n+1} = \mathop{\mathbf{A}}_{e=1}^{\text{Nel}}\left\{\int_{\Omega_e}\mathbf{B}^T(\mathbf{x})\cdot\mathbf{D}_T(\mathbf{x})\cdot\mathbf{B}(\mathbf{x})\cdot d\Omega_e\right\} \tag{10}$$

where $\mathbf{D}_T(\mathbf{x})$ denotes the matrix of material consistent or algorithmic tangent moduli obtained through consistent linearization of the numerical scheme used to integrate the rate constitutive equations (Simo and Hughes 1998). The above Netwon-Raphson procedure is represented schematically in Fig. 2. In the case of modified Newton, $(\mathbf{K}_T^{\text{stat}})^i_{n+1} = (\mathbf{K}_T^{\text{stat}})^0_{n+1}$, for all $i = 0,1,2,\ldots$. For Method II considered in this section, this numerical scheme for response calculation is then differentiated exactly with respect to the sensitivity parameter θ. Note that the semi-discrete (time continuous-spatially discrete) equations are not used at all in obtaining the sensitivity equations. Assuming that $\mathbf{u}_{n+1}$ is the converged solution (up to some iteration residuals satisfying a specified tolerance usually taken in the vicinity of the machine precision) for the current time step $[t_n, t_{n+1}]$, and differentiating Eq. (4) with respect to θ using the chain rule, recognizing that $\boldsymbol{\sigma} = \boldsymbol{\sigma}(\boldsymbol{\epsilon}(t,\theta),\theta)$ where $\boldsymbol{\sigma}$ and $\boldsymbol{\epsilon}$ denote the stress and strain tensors, respectively, we obtain

$$\left[\frac{1}{\beta(\Delta t)^2}\mathbf{M} + \frac{\alpha}{\beta(\Delta t)}\mathbf{C} + (\mathbf{K}_T^{\text{stat}})_{n+1}\right]\frac{\partial\mathbf{u}_{n+1}}{\partial\theta} = -\left(\frac{1}{\beta(\Delta t)^2}\frac{\partial\mathbf{M}}{\partial\theta} + \frac{\alpha}{\beta(\Delta t)}\frac{\partial\mathbf{C}}{\partial\theta}\right)\mathbf{u}_{n+1} - \left.\frac{\partial\mathbf{R}(\mathbf{u}_{n+1}(\theta),\theta)}{\partial\theta}\right|_{\mathbf{u}_{n+1}} + \frac{\partial\tilde{\mathbf{F}}_{n+1}}{\partial\theta} \tag{11}$$

where

$$\begin{aligned}\frac{\partial\tilde{\mathbf{F}}_{n+1}}{\partial\theta} = {} & \frac{\partial\mathbf{F}_{n+1}}{\partial\theta} + \frac{\partial\mathbf{M}}{\partial\theta}\left[\frac{1}{\beta(\Delta t)^2}\mathbf{u}_n + \frac{1}{\beta(\Delta t)}\dot{\mathbf{u}}_n - \left(1-\frac{1}{2\beta}\right)\ddot{\mathbf{u}}_n\right] \\ & + \mathbf{M}\left[\frac{1}{\beta(\Delta t)^2}\frac{\partial\mathbf{u}_n}{\partial\theta} + \frac{1}{\beta(\Delta t)}\frac{\partial\dot{\mathbf{u}}_n}{\partial\theta} - \left(1-\frac{1}{2\beta}\right)\frac{\partial\ddot{\mathbf{u}}_n}{\partial\theta}\right] \\ & + \frac{\partial\mathbf{C}}{\partial\theta}\left[\frac{\alpha}{\beta(\Delta t)}\mathbf{u}_n - \left(1-\frac{\alpha}{\beta}\right)\dot{\mathbf{u}}_n - (\Delta t)\left(1-\frac{\alpha}{2\beta}\right)\ddot{\mathbf{u}}_n\right] \\ & + \mathbf{C}\left[\frac{\alpha}{\beta(\Delta t)}\frac{\partial\mathbf{u}_n}{\partial\theta} - \left(1-\frac{\alpha}{\beta}\right)\frac{\partial\dot{\mathbf{u}}_n}{\partial\theta} - (\Delta t)\left(1-\frac{\alpha}{2\beta}\right)\frac{\partial\ddot{\mathbf{u}}_n}{\partial\theta}\right]\end{aligned} \tag{12}$$

The second term on the right-hand-side of Eq. (11) represents the partial derivative of the internal resisting force vector, $\mathbf{R}(\mathbf{u}_{n+1})$, with respect to sensitivity parameter θ under the condition that the displacement vector $\mathbf{u}_{n+1}$ remains fixed. From Eq. (5), this conditional derivative term can be expressed as

$$\left.\frac{\partial\mathbf{R}(\mathbf{u}_{n+1}(\theta),\theta)}{\partial\theta}\right|_{\mathbf{u}_{n+1}} = \mathop{\mathbf{A}}_{e=1}^{\text{Nel}}\int_{\Omega_e}\mathbf{B}^T(\mathbf{x})\cdot\left.\frac{\partial\boldsymbol{\sigma}(\mathbf{x})}{\partial\theta}\right|_{\boldsymbol{\epsilon}_{n+1}(\mathbf{x})}\cdot d\Omega_e \tag{13}$$

where $\partial\boldsymbol{\sigma}(\mathbf{x})/\partial\theta|_{\boldsymbol{\epsilon}_{n+1}(\mathbf{x})}$ denotes the derivative of the stress vector $\boldsymbol{\sigma}(\boldsymbol{\epsilon}_{n+1}(\theta),\theta)$ with respect to θ for fixed strain vector $\boldsymbol{\epsilon}_{n+1}$.

Analytical expressions for this history dependent conditional derivative of the stress vector have been derived by Zhang and Der Kiureghian (1993) and Conte and co-workers (1995, 1998) for the constitutive J_2 (or Von Mises) plasticity model and by

Conte and Jagannath (1995) and Conte et al. (1995) for the constitutive cap plasticity model in the case of a return map constitutive integration algorithm (Simo and Hughes 1998). Notice that once the numerical response of the system at t_{n+1} is known, the matrix sensitivity Eq. (11) is linear and has the same left-hand-side matrix operator as the consistently linearized Eq. (6) for the response at the last iteration before convergence is achieved for the current time step $[t_n, t_{n+1}]$. Therefore, only the right-hand-side of Eq. (6) needs to be recomputed and since the factorization of the tangent dynamic stiffness matrix $\mathbf{K}_T^{\text{dyn}}$ is already available (stored in the computer) at the converged time step t_{n+1}, solution of Eq. (11) is computationally cheap (only forward-backward substitution phase). This summarizes the steps for computing the response sensitivities using Method II. Some observations about Method II are made below.

Method II exactly differentiates the numerical time stepping scheme for computing the response sensitivities and, having made this identification, there is absolutely no confusion as to which tangent moduli (consistent or continuum) to use in building the static tangent stiffness matrix in Eq. (10). Differentiation of the numerical scheme for determining $\boldsymbol{\sigma}_{n+1}$ from $\boldsymbol{\epsilon}_{n+1}$ indeed provides the consistent tangent moduli. In this regard, some of the previous works mentioned earlier seem to be adopting Method I for arriving at the sensitivity equations which would naturally require using the continuum tangent as shown in the next section. Instead, they use the consistent tangent moduli as required by Method II. This clear distinction between the two approaches and the appropriateness of using either of the two tangent moduli seem to be lacking. Further, for viscoelastic and viscoplastic models (not considered in this paper) where the constitutive relations are given in terms of convolution integrals for history dependence (Simo and Hughes 1998), the notion of a continuum tangent does not even exist. For these cases, Method II is probably the only recourse. These situations make the distinction between the two methods all the more important.

Numerical Sensitivity of Exact Response (Method I)

This section briefly discusses the alternative approach where the semi-discrete (time continuous-spatially discrete) equations are used to obtain the response sensitivity equations. Differentiating exactly the semi-discretized nonlinear equation of motion (1) with respect to θ and changing the order of differentiation with respect to t and θ yields

$$\mathbf{M}(\theta)\ddot{\mathbf{v}}(t,\theta)+\mathbf{C}(\theta)\dot{\mathbf{v}}(t,\theta)+\tilde{\mathbf{K}}_T[\mathbf{u}(t,\theta)]\mathbf{v}(t,\theta) = \frac{\partial \mathbf{F}(t,\theta)}{\partial\theta}-\frac{\partial \mathbf{M}(\theta)}{\partial\theta}\ddot{\mathbf{u}}(t,\theta)-\frac{\partial \mathbf{C}(\theta)}{\partial\theta}\dot{\mathbf{u}}(t,\theta) - \frac{\partial}{\partial\theta}\mathbf{R}[\mathrm{u}(t,\theta),\theta]\bigg|_{\mathbf{u}} \tag{14}$$

where $\mathbf{v}(t,\theta)=\partial\mathbf{u}(t,\theta)/\partial\theta$ and $\tilde{\mathbf{K}}_T$ denotes the continuum (static) tangent stiffness matrix obtained from the continuum tangent moduli (when the notion of continuum tangent moduli exists) of the material. A sufficient condition for permuting the partial derivatives with respect to t and θ is that the partial derivatives $\partial\mathbf{u}/\partial\theta$, $\partial\mathbf{u}/\partial t$, and $\partial(\partial\mathbf{u}/\partial t)/\partial\theta$ exist and be continuous in both θ and t at all points along the time axis at $\theta=\theta_0$, the reference value of the sensitivity parameter (Courant 1988). However, in the case of inelastic systems, $\partial\mathbf{u}/\partial\theta$ and $\partial(\partial\mathbf{u}/\partial t)/\partial\theta$ are only piecewise continuous.

Both for Methods I and II, from a numerical standpoint, it can be assumed that the changes of material state occur within time steps and never exactly at the discrete time values considered by the time stepping scheme. The justification is that the probability of a material state transition occurring exactly at a discretized time value t_n, while performing the computations using double precision arithmetic is negligible (Kleiber et al. 1997). This implies that at any discrete time t_n, the material state and hence the tangent stiffness matrix are uniquely defined.

Furthermore, from a comparison of the two methods, one can enumerate the assumptions on Method I to obtain Method II. As mentioned in the Introduction, the lack of clear distinction between these two methods has led some earlier works to adopt Method I but make the following assumptions, which exactly leads one to Method II. These conditions can be listed as:

1. Integration of the semi-discretized governing sensitivity Eq. (14) over time step $[t_n, t_{n+1}]$ using the same time stepping scheme, see Eq. (3), as that for integrating the semi-discretized equation of motion given in Eq. (1);
2. Using the same constitutive law integration scheme (return map algorithm) for integrating the sensitivity equation as that used for integrating the response equation; and
3. Replacing the continuum (static) tangent stiffness matrix $\tilde{\mathbf{K}}_T$ by the consistent (static) tangent stiffness matrix $\mathbf{K}_T^{\text{stat}}$.

Although the above Conditions 1 and 2 are justifiable, Condition 3 is very ad hoc simply because the consistent tangent stiffness is purely an outcome of discretizing the response equations in space and in time and then differentiating the resulting numerical scheme. These conditions establish the equivalence between the two methods and help clarify some of the earlier works.

Discontinuities due to Material State Transitions

The response sensitivity of an inelastic dynamic system, $\partial r(t)/\partial\theta\big|_{\theta=\theta_0}$, is not continuous in time as illustrated in Fig. 3(c) for the case in which $r(t)$ is taken as a nodal displacement response $u(t)$. The discontinuities along the time axis arise due to a finite number of switchings between material states, i.e., switching between elastic and plastic states and vice-versa (Kleiber et al. 1997; Conte and Vijalapura 1998; Conte 2001). The governing sensitivity Eq. (11) involves the partial derivative $\partial/\partial\theta$ of the internal resisting force vector $\mathbf{R}$, which changes with change in material state for a given deformation state, thus in general producing discontinuities in the sensitivity of the nodal displacement responses (see the section ''Propagation of Discontinuities from Local to Global Response Sensitivities''). The exact instants in time t', t'', and t''' in Fig. 3 depict these material switching times. At the material state transition points, the response sensitivity is undefined as shown in Fig. 3, the values of the sensitivity being different for the two material states immediately preceding and succeeding the exact transition time. Hence, numerical algorithms used to compute response sensitivities must be able to capture these discontinuities.

In solving the nonlinear equations of motion using the Newton-Raphson (or even modified Newton) incremental-iterative procedure in conjunction with a return map algorithm (Simo and Hughes 1998) to integrate the rate constitutive equations, the exact time (within a time step) at which a material state transition occurs is not explicitly solved for. If it were the case, this exact time would have to be differentiated with respect to the sensitivity parameter θ (Conte and Vijalapura 1998) in order to carry the discontinuity of the response sensitivity across the change of material state. In the case of a return map constitutive

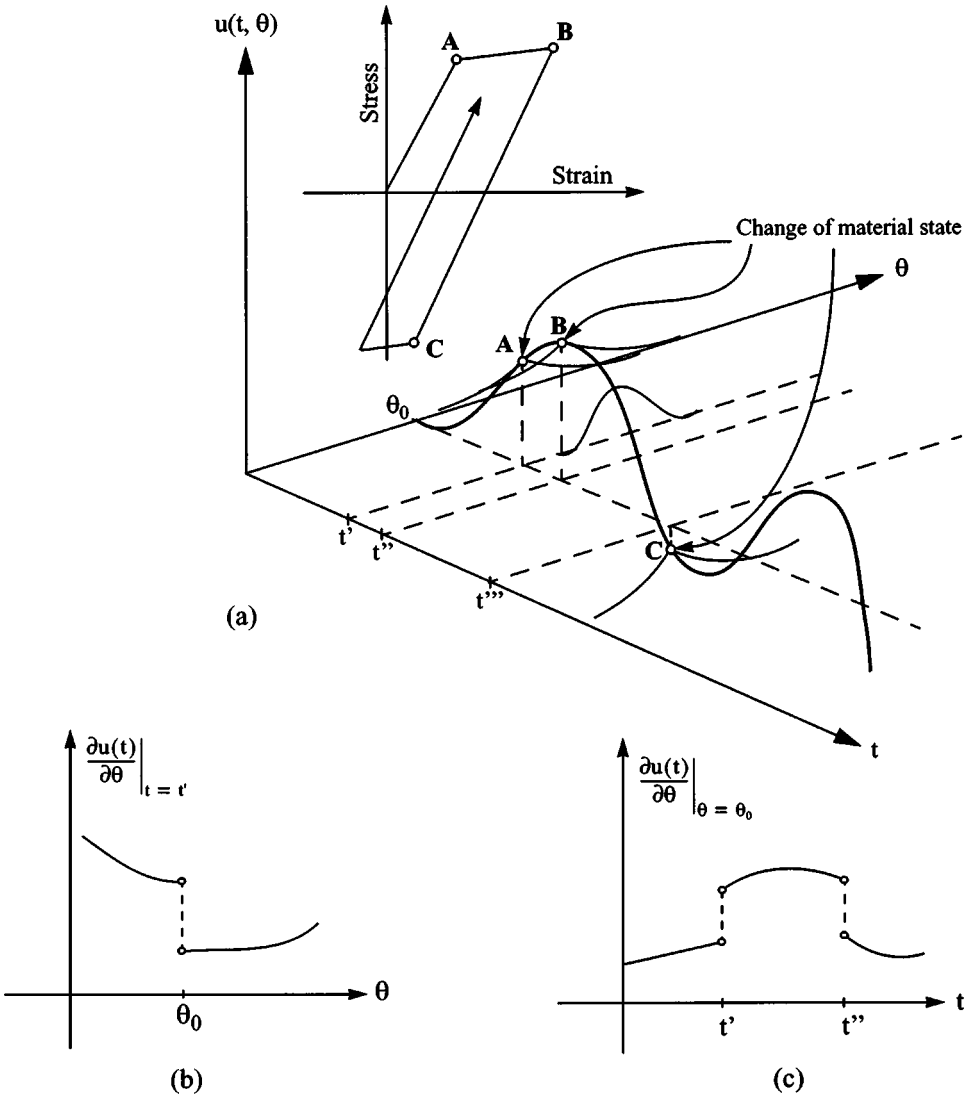

Fig. 3. Sketch of discontinuities in displacement response sensitivity

integration algorithm and assuming that a material state transition occurs at a Gauss quadrature point within the time step $[t_n, t_{n+1}]$, the corresponding discontinuities in the derivatives of the history/state variables (e.g., plastic strain components, hardening parameter, etc.) are captured by the differentiation algorithm outlined above (i.e., Method II), although the exact occurrence time within a time step of the material state transition is not solved for. Thus, the discontinuities in the derivatives with respect to material and loading parameters of global response quantities are carried consistently across material state transitions through the upward (from local/Gauss point level to global/structure level) propagation of the discontinuities in derivatives of history variables at the element (or Gauss point) level. All these ideas are made concrete through an example one-dimensional (1D) plasticity model below.

Finite-Element Implementation and Validation of Method II

The procedure for consistent finite element response sensitivity analysis presented as Method II (or consistent DDM) requires extensions of standard nonlinear finite-element analysis codes in order to compute and assemble the finite-element contributions to the right-hand-side of the sensitivity Eq. (11) and solve the latter. This procedure was implemented in the general-purpose nonlinear finite-element analysis program *FEAP* developed by Taylor (1998) (Zienkiewicz and Taylor 2000) and validated through various examples in which the exact sensitivities of the computed hysteretic finite-element response are validated through finite difference sensitivity calculations (Conte and Jagannath 1995; Conte et al. 1995; Conte and Vijalapura 1998; Conte 2001). The interested reader is referred to the above references for further details on the development of the above procedure (Method II) for both the J_2 (von Mises) and cap plasticity models, its software implementation and validation.

Example of One-Dimensional J_2 (von Mises) Plasticity

This section particularizes the various steps in Method II to a simple 1D J_2 Plasticity model with the von Mises yield criterion. The equations for the numerical integration of the rate constitutive relations of the 1D model, for both the response and response sensitivities are provided below. For the multidimensional J_2 plasticity model as well as the more complicated cap plasticity model, the reader is referred elsewhere (Conte and Jagannath 1995; Conte et al. 1995; Conte and Vijalapura 1998; Conte 2001).

The plasticity model assumes that the 1D total strain ε can be additively split into an elastic part ε^e and a plastic part ε^p. The 1D stress σ depends only on ε^e. Plasticity is introduced through a scalar yield function $f(\sigma,\alpha,\bar{\varepsilon}^p)$ in the stress space. Here, the scalar α is called the back-stress and models the kinematic hardening, while $\bar{\varepsilon}^p$ is the cumulative plastic strain and is used as isotropic hardening parameter. The elastic domain is defined by states of stress such that $f(\sigma,\alpha,\bar{\varepsilon}^p)<0$ and the yield function is constrained to take on nonpositive values, i.e., $f(\sigma,\alpha,\bar{\varepsilon}^p)\leqslant 0$. When the state of stress is on the yield surface, i.e., $f(\sigma,\alpha,\bar{\varepsilon}^p)=0$, plastic flow (described by the flow rule), or elastic unloading takes place depending on the total strain rate $\dot{\varepsilon}$, either being determined uniquely by the plastic consistency condition or the Kuhn-Tucker conditions for loading/unloading and the plastic consistency equation (Simo and Hughes 1998). The hardening of the material during yielding is modeled by the hardening law. The equations for the 1D J_2 plasticity model with von Mises yield function and a linear hardening law are summarized below.

1. Additive decomposition of the total strain

$$\varepsilon=\varepsilon^e+\varepsilon^p \tag{15}$$

2. Elastic stress-strain relations

$$\sigma=E\cdot\varepsilon^e \tag{16}$$

where E=elastic Young's modulus of the material;

3. Flow rule

$$\dot{\varepsilon}^p=\dot{\lambda}\cdot\mathrm{sgn}(\sigma-\alpha) \tag{17}$$

where $\dot{\lambda}$=consistency parameter and sgn(...) denotes the sign function;

4. Hardening laws (linear kinematic and linear isotropic hardening)

$$\dot{\alpha}=H_{\mathrm{kin}}\cdot\dot{\varepsilon}^p$$

$$\dot{\bar{\varepsilon}}^p=\dot{\lambda} \tag{18}$$

$$\sigma_y=\sigma_{y0}+H_{\mathrm{iso}}\cdot\bar{\varepsilon}^p$$

where $\dot{\bar{\varepsilon}}^p=\sqrt{\dot{\varepsilon}^p}=|\dot{\varepsilon}^p|$ denotes the rate of effective plastic strain, $\bar{\varepsilon}^p=\int_0^t\dot{\bar{\varepsilon}}^p\cdot dt$=effective or cumulative plastic strain; σ_{y0}=initial yield stress; σ_y=current yield stress; and H_{kin} and H_{iso}=kinematic and isotropic hardening moduli, respectively;

5. Kuhn-Tucker conditions for loading/unloading

$$\dot{\lambda}\geqslant 0,\quad f(\sigma,\alpha,\bar{\varepsilon}^p)\leqslant 0\quad\text{and}\quad\dot{\lambda}\cdot f=0 \tag{19}$$

6. Plastic consistency condition

$$\dot{\lambda}\geqslant 0,\quad \dot{f}(\sigma,\alpha,\bar{\varepsilon}^p)\leqslant 0\quad\text{and}\quad\dot{\lambda}\cdot\dot{f}=0 \tag{20}$$

The yield function is of the form

$$f(\sigma,\alpha,\bar{\varepsilon}^p)=|\sigma-\alpha|-(\sigma_{y0}+H_{\mathrm{iso}}\bar{\varepsilon}^p) \tag{21}$$

The 1D J_2 plasticity model with pure linear kinematic hardening ($H_{\mathrm{iso}}=0$) corresponds to the well-known bilinear inelastic model shown in Fig. 4. In the above, the flow rule and hardening laws are given in rate form. The rate constitutive equations have to be integrated numerically in order to obtain the stress history for a given strain history. Using the implicit backward Euler scheme to time-discretize the rate equations over the time step $[t_n,t_{n+1}]$ (with step size $\Delta t=t_{n+1}-t_n$), we obtain the following discretized material constitutive equations:

1. Additive split of the total strain

$$\varepsilon_{n+1}=\varepsilon^e_{n+1}+\varepsilon^p_{n+1} \tag{22}$$

2. Elastic stress-strain relation

$$\sigma_{n+1}=E\cdot\varepsilon^e_{n+1} \tag{23}$$

3. Flow rule

$$\varepsilon^p_{n+1}=\varepsilon^p_n+\Delta\lambda\cdot\mathrm{sgn}(\sigma_{n+1}-\alpha_{n+1}) \tag{24}$$

where $\Delta\lambda=\int_{t_n}^{t_{n+1}}\dot{\lambda}\cdot dt\cong\dot{\lambda}_{n+1}\cdot\Delta t$ is the discrete consistency parameter;

4. Hardening laws (linear kinematic and linear isotropic hardening)

$$\alpha_{n+1}=\alpha_n+H_{\mathrm{kin}}\cdot\Delta\lambda\cdot\mathrm{sgn}(\sigma_{n+1}-\alpha_{n+1})$$

$$\bar{\varepsilon}^p_{n+1}=\bar{\varepsilon}^p_n+\Delta\lambda \tag{25}$$

$$\sigma_{y,n+1}=\sigma_{y,n}+H_{\mathrm{iso}}\cdot\Delta\lambda$$

5. Kuhn-Tucker loading/unloading and plastic consistency conditions

$$\Delta\lambda\geqslant 0,\quad f(\sigma_{n+1},\alpha_{n+1},\bar{\varepsilon}^p_{n+1})\leqslant 0$$

and

$$\Delta\lambda\cdot f(\sigma_{n+1},\alpha_{n+1},\bar{\varepsilon}^p_{n+1})=0 \tag{26}$$

The subscript $(\ldots)_{n+1}$ denotes that the quantity to which the subscript is attached is evaluated at time t_{n+1}.

As a particular one-dimensional application of the very effective elastic-plastic operator split method with a concept of return map which is based on the notion of closest-point-projection in the stress space (Simo and Hughes 1998), the above discretized constitutive equations are solved for stress component σ_{n+1} in two steps, namely (1) a trial elastic step and (2) a plastic corrector step. In the trial elastic step, the plastic response is frozen and, consequently, all of the current total strain increment ($\Delta\varepsilon_{n+1}=\varepsilon_{n+1}-\varepsilon_n$) is assumed to be elastic. If the stress computed under this assumption satisfies the yield condition, then the current step is elastic and the integration of the material constitutive law over time step $[t_n,t_{n+1}]$ is complete. Otherwise, the above discrete constitutive equations are solved for the discrete consistency parameter $\Delta\lambda$ and finally for σ_{n+1} (by the return map algorithm). The procedure is summarized below.

Trial Elastic State

$$\begin{gathered}\Delta\lambda^{\mathrm{Trial}}=0\\ (\varepsilon^p_{n+1})^{\mathrm{Trial}}=\varepsilon^p_n\\ \alpha^{\mathrm{Trial}}_{n+1}=\alpha_n\\ (\bar{\varepsilon}^p_{n+1})^{\mathrm{Trial}}=\bar{\varepsilon}^p_n\\ \sigma^{\mathrm{Trial}}_{n+1}=\mathrm{E}(\varepsilon_{n+1}-\varepsilon^p_n)\\ \sigma^{\mathrm{Trial}}_{y,n+1}=\sigma_{y,n}\end{gathered} \tag{27}$$

IF $\{f(\sigma^{\mathrm{Trial}}_{n+1},\alpha^{\mathrm{Trial}}_{n+1},(\bar{\varepsilon}^p_{n+1})^{\mathrm{Trial}})\leqslant 0\}$ THEN

Update all the state/history variables at time t_{n+1} by assigning the corresponding trial values to them, i.e., $(\ldots)_{n+1}=(\ldots)^{\mathrm{Trial}}_{n+1}$ and EXIT.

ELSE

Plastic Corrector Step Using the Return Map Algorithm

The plastic corrector step is based upon satisfying the consistency condition in discrete form

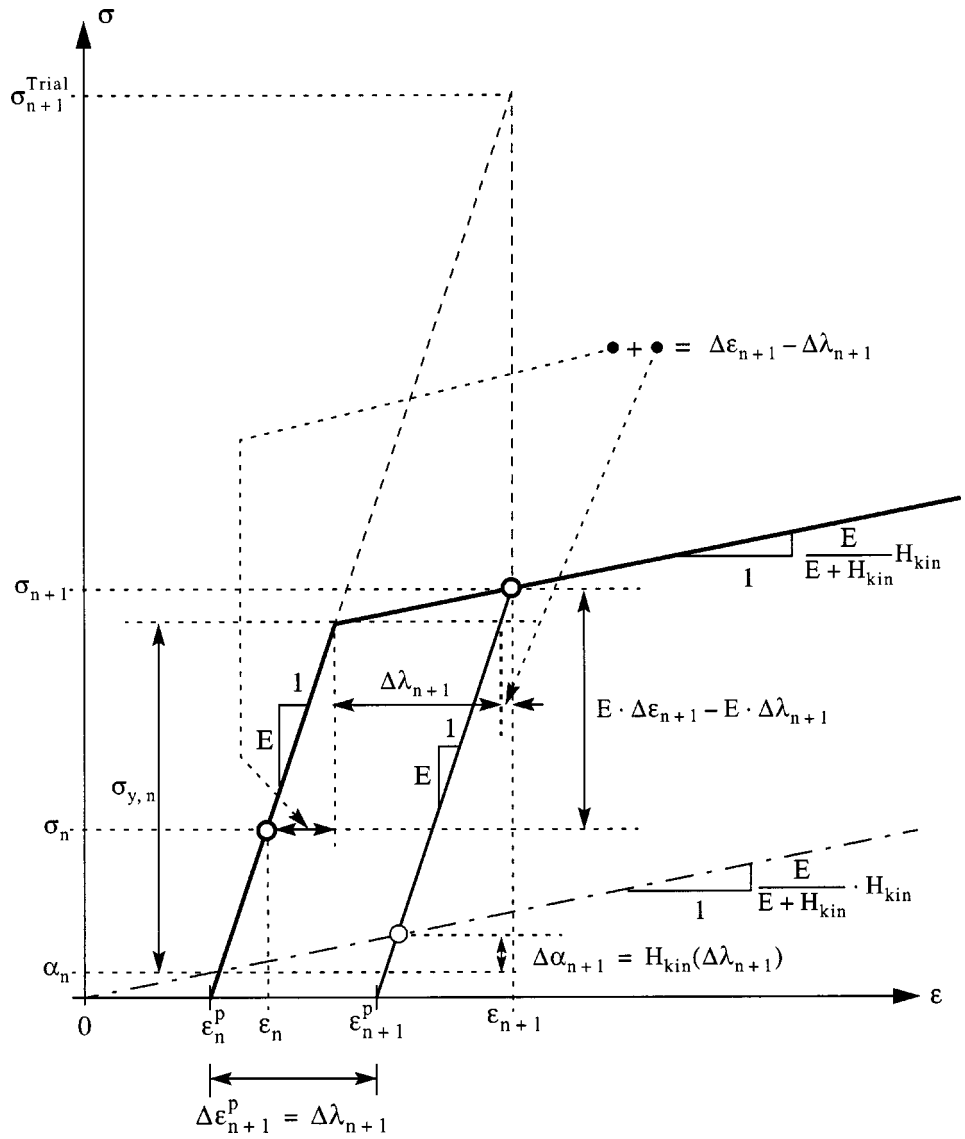

Fig. 4. Return map algorithm for 1D J_2 (von Mises) plasticity model with pure kinematic hardening ($H_{\text{iso}}=0$)

$$f_{n+1}=|\sigma_{n+1}-\alpha_{n+1}|-\sigma_{y,n+1}=0 \tag{28}$$

where

$$\begin{aligned}\sigma_{n+1}&=E(\varepsilon_{n+1}-\varepsilon^p_{n+1})\\&=E\{\varepsilon_{n+1}-\varepsilon^p_n-[\Delta\lambda\cdot\operatorname{sgn}(\sigma_{n+1}-\alpha_{n+1})]\}\\&=\sigma^{\text{Trial}}_{n+1}-E\cdot\Delta\lambda\cdot\operatorname{sgn}(\sigma_{n+1}-\alpha_{n+1})\end{aligned} \tag{29}$$

$$\begin{aligned}\alpha_{n+1}&=\alpha_n+H_{\text{kin}}\cdot\Delta\lambda\cdot\operatorname{sgn}(\sigma_{n+1}-\alpha_{n+1})\\&=\alpha^{\text{Trial}}_{n+1}+H_{\text{kin}}\cdot\Delta\lambda\cdot\operatorname{sgn}(\sigma_{n+1}-\alpha_{n+1})\end{aligned} \tag{30}$$

$$\sigma_{y,n+1}=\sigma_{y,n}+H_{\text{iso}}\cdot\Delta\lambda \tag{31}$$

Using the expressions for σ_{n+1} and α_{n+1} in Eqs. (29) and (30) and defining

$$n_{n+1}=\frac{\sigma_{n+1}-\alpha_{n+1}}{|\sigma_{n+1}-\alpha_{n+1}|}=\operatorname{sgn}(\sigma_{n+1}-\alpha_{n+1}) \tag{32}$$

we obtain

$$\begin{aligned}\sigma_{n+1}-\alpha_{n+1}&=|\sigma_{n+1}-\alpha_{n+1}|\cdot n_{n+1}\\&=(\sigma^{\text{Trial}}_{n+1}-\alpha^{\text{Trial}}_{n+1})-(E+H_{\text{kin}})\cdot\Delta\lambda\cdot n_{n+1}\end{aligned} \tag{33}$$

By analyzing the signs of the three terms of the equation formed by the second equal sign in Eq. (33), it follows that

$$\operatorname{sgn}(\sigma_{n+1}-\alpha_{n+1})=\operatorname{sgn}(\sigma^{\text{Trial}}_{n+1}-\alpha^{\text{Trial}}_{n+1})=n_{n+1} \tag{34}$$

and

$$|\sigma_{n+1}-\alpha_{n+1}|=|\sigma^{\text{Trial}}_{n+1}-\alpha^{\text{Trial}}_{n+1}|-(E+H_{\text{kin}})\Delta\lambda \tag{35}$$

Therefore, using Eq. (31), we can write the discrete consistency condition in Eq. (28) as

$$|\sigma^{\text{Trial}}_{n+1}-\alpha^{\text{Trial}}_{n+1}|-(E+H_{\text{kin}})\cdot\Delta\lambda-\sigma_{y,n}-H_{\text{iso}}\cdot\Delta\lambda=0 \tag{36}$$

The discrete consistency parameter $\Delta\lambda$ can be obtained from the above equation as

$$\Delta\lambda=\frac{|\sigma^{\text{Trial}}_{n+1}-\alpha^{\text{Trial}}_{n+1}|-\sigma_{y,n}}{E+H_{\text{iso}}+H_{\text{kin}}} \tag{37}$$

Given ε_{n+1} and once $\Delta\lambda$ is known, the state/history variables at t_{n+1} (i.e., ε^p_{n+1}, σ_{n+1}, α_{n+1}, $\overline{\varepsilon^p}_{n+1}$, $\sigma_{y,n+1}$) are obtained from Eqs. (24), (25), and (29). The above discrete constitutive integration scheme for 1D J_2 plasticity is represented graphically in Fig. 4 for a plastic step.

Response Sensitivity Calculations

It was shown earlier that the formation of the response sensitivity equation, Eq. (11), requires computation of the derivative $d\sigma_{n+1}/d\varepsilon_{n+1}$ in order to evaluate the consistent (or algorithmic) tangent stiffness matrix $\mathbf{K}_T^{\text{stat}}=\partial\mathbf{R}/\partial\mathbf{u}$. Also, the term $\partial\sigma_{n+1}/\partial\theta\big|_{\varepsilon_{n+1}}$ needs to be computed in order to evaluate the term $\partial\mathbf{R}/\partial\theta\big|_{\mathbf{u}}$ in the right-hand-side of the response sensitivity Eq. (11). In the context of Method II, the derivative $d\sigma_{n+1}/d\varepsilon_{n+1}$ relates the infinitesimal incremental change in the stress σ_{n+1} computed *algorithmically* (according to the return map algorithm in our case) to an infinitesimal incremental change in the value of the total strain ε_{n+1} at time t_{n+1}, while keeping fixed all other state/history variables at time t_n that appear in the material constitutive integration algorithm. We differentiate the discrete constitutive integration algorithm (i.e., here return map algorithm) to compute the derivative $d\sigma_{n+1}/d\varepsilon_{n+1}$. When the current step is elastic, $\varepsilon^p_{n+1}=(\varepsilon^p_{n+1})^{\text{Trial}}=\varepsilon^p_n$, and taking differentials on both sides of Eq. (27) yields $d\sigma_{n+1}=E\cdot d\varepsilon_{n+1}$. When the current step is plastic, we use the equations for the plastic corrector step. Taking differentials on both sides of Eqs. $(29)_1$ and (24), and using Eq. (34) and $dn_{n+1}=0$ (since the sign function is either $+1$ or -1 and, in finite precision arithmetic, we are never at the point of discontinuity of the sign function), we have

$$d\sigma_{n+1}=E\cdot(d\varepsilon_{n+1}-d\varepsilon^p_{n+1}) \tag{38}$$

and

$$d\varepsilon^p_{n+1}=d(\Delta\lambda)\cdot n_{n+1} \tag{39}$$

The discrete consistency parameter $\Delta\lambda$ is obtained from the discrete consistency condition in Eq. (28). Thus, taking differentials on both sides of the discrete consistency condition, using Eqs. $(29)_1$, $(30)_1$, (31), and the identity $n_{n+1}\cdot n_{n+1}=1$ yields

$$\begin{aligned} df_{n+1}&=d|\sigma_{n+1}-\alpha_{n+1}|-d\sigma_{y,n+1}=0\\ &=d(\sigma_{n+1}-\alpha_{n+1})n_{n+1}-d\sigma_{y,n+1}=0\\ &=E(d\varepsilon_{n+1}-d\varepsilon^p_{n+1})n_{n+1}-H_{\text{kin}}\cdot d(\Delta\lambda)-H_{\text{iso}}\cdot d(\Delta\lambda) \end{aligned} \tag{40}$$

Multiplying last equation by n_{n+1} and using the expression in Eq. (39) for $d\varepsilon^p_{n+1}$, we obtain

$$d(\Delta\lambda)=\left(\frac{E}{E+H_{\text{kin}}+H_{\text{iso}}}\right)\cdot d\varepsilon_{n+1}\cdot n_{n+1} \tag{41}$$

Substituting Eqs. (39) and (41) into Eq. (38) yields

$$d\sigma_{n+1}=E\cdot\left(1-\frac{E}{E+H_{\text{kin}}+H_{\text{iso}}}\right)\cdot d\varepsilon_{n+1} \tag{42}$$

which relates the infinitesimal incremental stress computed algorithmically to an infinitesimal incremental strain. Therefore, in the case of the 1D J_2 plasticity model, the consistent (or algorithmic) elastoplastic material tangent modulus is given by

$$D_T=E\cdot\left(1-\frac{E}{E+H_{\text{kin}}+H_{\text{iso}}}\right)=\frac{H_{\text{kin}}+H_{\text{iso}}}{E+H_{\text{kin}}+H_{\text{iso}}}\cdot E \tag{43}$$

which is shown in Fig. 4 in the case of pure kinematic hardening ($H_{\text{iso}}=0$) and corresponds to the post-yield stiffness of the bilinear inelastic model. Thus, in the present case, the consistent material tangent modulus is identical to the continuum tangent modulus. It can be shown that for the one-dimensional case, the consistent (or algorithmic) tangent modulus coincides with the continuum elastoplastic tangent modulus irrespective of the constitutive plasticity model. However, this result does not hold for the multidimensional case in which strains, stresses, and material tangent moduli are tensorial quantities (Simo and Hughes 1998). In the multidimensional case, for large time steps, the consistent tangent moduli may differ significantly from the ''continuum'' ones (Conte and Jagannath 1995; Conte and Vijalapura 1998; Simo and Hughes 1998).

Consider the conditional derivative of a generic state/history variable, $\partial(\ldots)/\partial\theta\big|_{\mathbf{u}}$. In displacement-based finite-element analysis, fixing the displacement $\mathbf{u}(t_{n+1})=\mathbf{u}_{n+1}$ is equivalent to fixing the strain ε_{n+1}. Therefore, the conditional derivatives of the state/history variables are simply obtained by substituting with zero all the occurrences of the derivative $\partial\varepsilon_{n+1}/\partial\theta$ in the expressions for the (unconditional) derivatives of the state/history variables, $\partial(...)/\partial\theta$.

If no plastic deformation takes place during the current time step $[t_n,t_{n+1}]$, the trial solutions for the state variables given by the elastic predictor step are also the correct solutions, i.e., the elastic predictor step is not followed by a plastic corrector step. Hence, dropping the superscript ''Trial'' from Eqs. (27) and differentiating them with respect to the sensitivity parameter θ, we obtain

$$\frac{\partial}{\partial\theta}(\Delta\lambda)=0 \tag{44}$$

$$\frac{\partial\varepsilon^p_{n+1}}{\partial\theta}=\frac{\partial\varepsilon^p_n}{\partial\theta} \tag{45}$$

$$\frac{\partial\alpha_{n+1}}{\partial\theta}=\frac{\partial\alpha_n}{\partial\theta} \tag{46}$$

$$\frac{\partial\overline{\varepsilon^p}_{n+1}}{\partial\theta}=\frac{\partial\overline{\varepsilon^p}_n}{\partial\theta} \tag{47}$$

$$\frac{\partial\sigma_{n+1}}{\partial\theta}=E\left(\frac{\partial\varepsilon_{n+1}}{\partial\theta}-\frac{\partial\varepsilon^p_n}{\partial\theta}\right)+\frac{\partial\mathrm{E}}{\partial\theta}(\varepsilon_{n+1}-\varepsilon^p_n) \tag{48}$$

$$\frac{\partial\sigma_{y,n+1}}{\partial\theta}=\frac{\partial\sigma_{y,n}}{\partial\theta} \tag{49}$$

If plastic deformation takes place during the current step $[t_n,t_{n+1}]$, the elastoplastic constitutive relations in the discrete form are differentiated exactly with respect to the sensitivity parameter θ in order to compute the derivatives of the state/history variables at t_{n+1}. Differentiating Eq. $(29)_1$ with respect to θ produces

$$\frac{\partial\sigma_{n+1}}{\partial\theta}=E\cdot\left(\frac{\partial\varepsilon_{n+1}}{\partial\theta}-\frac{\partial\varepsilon^p_{n+1}}{\partial\theta}\right)+\frac{\partial E}{\partial\theta}\cdot(\varepsilon_{n+1}-\varepsilon^p_{n+1}) \tag{50}$$

The derivative $\partial\varepsilon^p_{n+1}/\partial\theta$ is obtained by differentiating Eq. (24) with respect to θ, using Eq. (32), as

$$\frac{\partial\varepsilon^p_{n+1}}{\partial\theta}=\frac{\partial\varepsilon^p_n}{\partial\theta}+\frac{\partial(\Delta\lambda)}{\partial\theta}\cdot n_{n+1} \tag{51}$$

where again the derivative of n_{n+1} with respect to sensitivity parameter θ is set to zero. Using Eq. (34), Eq. (37) takes the form

$$\Delta\lambda = \frac{|\sigma_{n+1}^{\text{Trial}} - \alpha_{n+1}^{\text{Trial}}| - \sigma_{y,n}}{E + H_{\text{iso}} + H_{\text{kin}}} = \frac{(\sigma_{n+1}^{\text{Trial}} - \alpha_{n+1}^{\text{Trial}}) \cdot n_{n+1} - \sigma_{y,n}}{E + H_{\text{iso}} + H_{\text{kin}}} \tag{52}$$

Differentiating Eq. (52) with respect to θ yields

$$\frac{\partial(\Delta\lambda)}{\partial\theta} = \frac{(E + H_{\text{iso}} + H_{\text{kin}}) \cdot \left[\left(\frac{\partial \sigma_{n+1}^{\text{Trial}}}{\partial\theta} - \frac{\partial \alpha_n}{\partial\theta} \right) \cdot n_{n+1} - \frac{\partial \sigma_{y,n}}{\partial\theta} \right]}{(E + H_{\text{iso}} + H_{\text{kin}})^2} - \frac{\left(\frac{\partial E}{\partial\theta} + \frac{\partial H_{\text{iso}}}{\partial\theta} + \frac{\partial H_{\text{kin}}}{\partial\theta} \right) \cdot [(\sigma_{n+1}^{\text{Trial}} - \alpha_n) \cdot n_{n+1} - \sigma_{y,n}]}{(E + H_{\text{iso}} + H_{\text{kin}})^2} \tag{53}$$

where the derivative of $\sigma_{n+1}^{\text{Trial}}$ with respect to θ is obtained, using Eq. $(27)_5$, as

$$\frac{\partial \sigma_{n+1}^{\text{Trial}}}{\partial\theta} = E \cdot \left(\frac{\partial \varepsilon_{n+1}}{\partial\theta} - \frac{\partial \varepsilon_n^p}{\partial\theta} \right) + \frac{\partial E}{\partial\theta} \cdot (\varepsilon_{n+1} - \varepsilon_n^p) \tag{54}$$

The derivatives of the remaining state/history variables, $\overline{\varepsilon^p}_{n+1}$, $\sigma_{y,n+1}$, and α_{n+1}, with respect to the sensitivity parameter θ are obtained by differentiating Eqs. (25) as

$$\frac{\partial \overline{\varepsilon^p}_{n+1}}{\partial\theta} = \frac{\partial \overline{\varepsilon^p}_n}{\partial\theta} + \frac{\partial(\Delta\lambda)}{\partial\theta} \tag{55}$$

$$\frac{\partial \sigma_{y,n+1}}{\partial\theta} = \frac{\partial \sigma_{y,n}}{\partial\theta} + \frac{\partial H_{\text{iso}}}{\partial\theta} \cdot \Delta\lambda + H_{\text{iso}} \cdot \frac{\partial(\Delta\lambda)}{\partial\theta} \tag{56}$$

$$\frac{\partial \alpha_{n+1}}{\partial\theta} = \frac{\partial \alpha_n}{\partial\theta} + \frac{\partial H_{\text{kin}}}{\partial\theta} \cdot (\Delta\lambda) \cdot n_{n+1} + H_{\text{kin}} \cdot \frac{\partial(\Delta\lambda)}{\partial\theta} \cdot n_{n+1} \tag{57}$$

The conditional derivative $\partial \mathbf{R}/\partial\theta|_{\mathbf{u}}$ in the response sensitivity Eq. (11) at the structure level requires computation of the conditional derivative $\partial \sigma_{n+1}/\partial\theta|_{\mathbf{u}}$ at each Gauss quadrature point of the finite-element model of the structure. As mentioned earlier, this is achieved by substituting $\partial \varepsilon_{n+1}/\partial\theta$ with zero in Eqs. (50), (51), (53), and (54).

Propagation of Discontinuities from Local to Global Response Sensitivities

We shall examine the propagation of discontinuities in the response sensitivities for the simple 1D J_2 plasticity model considered here. During the response computation, each time step is either an elastic step or a plastic step depending on whether there is plastic flow or not. Correspondingly, Eqs. (44)–(49) are used to compute sensitivities for an elastic step, while Eqs. (50)–(57) are used for a plastic step. For this plasticity model, the discontinuities propagate starting with discontinuities in $\partial(\Delta\lambda)/\partial\theta$. The derivative $\partial(\Delta\lambda)/\partial\theta$ is zero for an elastic step, is given by Eq. (53) for a plastic step, and it jumps from zero to a nonzero value and vice-versa during elastic-to-plastic and plastic-to-elastic material state transitions, respectively. These discontinuities in $\partial(\Delta\lambda)/\partial\theta$ at the local (Gauss quadrature point) level propagate into discontinuities in the sensitivities of the stress σ, plastic strain ε^p, effective or cumulative plastic strain $\overline{\varepsilon^p}$, current yield stress σ_y, and back-stress α through Eqs. (50)–(57). Then, these discontinuities in response sensitivities at the local (Gauss quadrature point) level propagate mathematically and physically upwards into discontinuities in response sensitivities at the element level (e.g., element internal forces and deformations) and finally at the structure level (e.g., nodal displacement, base shear, etc.).

The propagation of discontinuities from local to global response sensitivities is illustrated through a simple application example, namely, a single degree-of-freedom (SDOF) elastoplastic system subjected to ground motion excitation as shown in Fig. 5. The input ground acceleration history $\ddot{u}_g(t)$ and displacement response history $u(t)$ are shown in Figs. 6(a and b), respectively. The reason why the input ground acceleration looks analytical with some small irregularities is that it was retrieved as one of the final iterations to find the design point during a time-variant reliability analysis of this elastoplastic SDOF system subjected to random ground motion excitation (Conte and Vijalapura 1998; Vijalapura et al. 1999). The sensitivities of the cumulative plastic strain, $\overline{\varepsilon^p}(t)$, and displacement $u(t)$ response histories with respect to the initial yield stress σ_{y_0} are shown in Figs. 7 and 8 (in

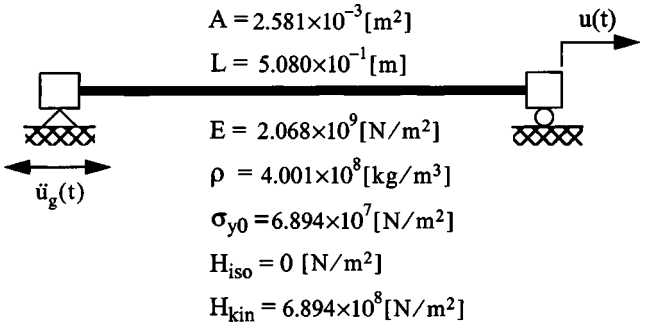

Fig. 5. SDOF system: Elastoplastic truss element

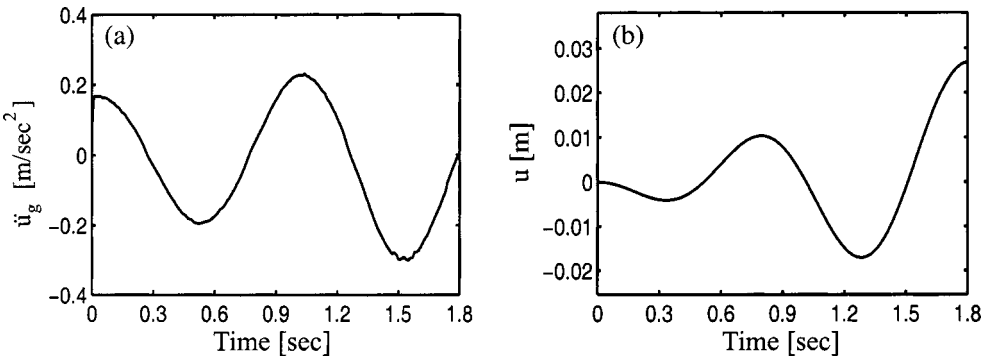

Fig. 6. (a) Input ground acceleration history and (b) displacement response history

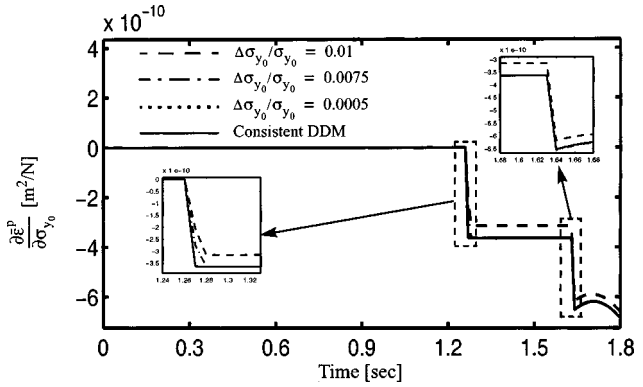

Fig. 7. Discontinuities in sensitivity of cumulative plastic strain response history to initial yield stress, σ_{y0}, due to material state transitions

solid line), respectively. Method II (consistent direct differentiation method) is adopted for the response sensitivity calculations. Figs. 7 and 8 also contain response sensitivity results (in dashed, dashed-dot, and dotted lines) obtained from forward finite difference analysis with decreasing values of the initial yield stress variation $\Delta\sigma_y$. It is observed that the finite difference results approach asymptotically the results obtained using the consistent DDM as further evidenced by the zoom views of the discontinuities shown in the insets of Figs. 7 and 8. As already mentioned, each discontinuity occurs somewhere within a time step and its exact time of occurrence is not explicitly solved for using the direct differentiation method. However, the values of the response sensitivities at both ends of the time step are in agreement with the finite difference results, thus indicating that the discontinuities in response sensitivities are consistently carried across the material state transitions.

In Fig. 7, the sensitivity of the cumulative plastic strain exhibits two discontinuities corresponding to a plastic loading in time step 1.26–1.27 s and a second plastic loading in time step 1.63–1.64 s. The first plastic loading is immediately followed by an elastic unloading. The discontinuities in the sensitivity of the discrete consistency parameter $\Delta\lambda$ with respect to σ_{y_0} propagate upward resulting in discontinuities in the sensitivity of the cumulative plastic strain, $\bar{\varepsilon}^p(t)$, and other state/history variables and finally in discontinuities in the sensitivity of the displacement response $u(t)$ at the structure level, as seen in Figs. 7 and 8.

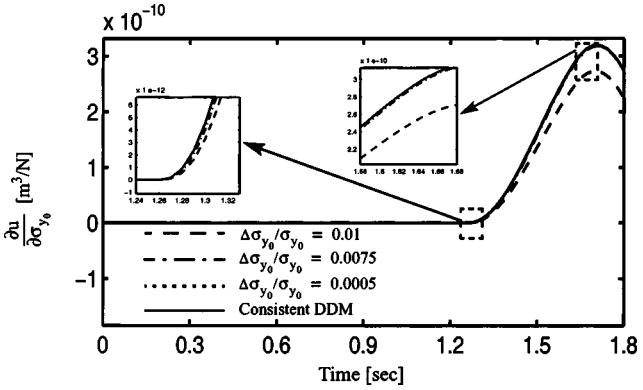

Fig. 8. Discontinuities in sensitivity of displacement response history to initial yield stress, σ_{y0}, due to material state transitions

Notice that the discontinuities in response sensitivities are very visible/pronounced at the local (Gauss quadrature point) level (Fig. 7), while they are not very apparent at the structure level (Fig. 8) where they are relatively much smaller and hidden or "smeared out" within the dynamics (time variation) of the response. Indeed, the response sensitivity plots are obtained by linearly interpolating the sensitivity values obtained at discrete times, and when a discontinuity within a time step is small, this discontinuity is not clearly resolved as in Fig. 8. In quasistatic elastoplastic problems, the discontinuities in response sensitivities at the structure level are much more visible (Conte 2001).

From the analysis provided here, material state transitions cause discontinuities in: (1) the derivatives (conditional and unconditional) of the internal resisting force vector, and (2) the consistent tangent stiffness matrix, in the response sensitivity Eq. (11). Therefore, the question naturally arises whether the discontinuity in the derivative of the internal resisting force vector [on the right-hand side of the sensitivity equation] can be counteracted by the discontinuity in the consistent tangent moduli from which the consistent tangent stiffness matrix is built [on the left-hand side of the sensitivity equation], resulting in continuous derivatives of the nodal displacements. From a mathematical point of view, a priori there is no reason to believe that there is a counteracting effect which keeps the sensitivity of the nodal displacements continuous in time. However, in some simple examples involving truss elements and beam elements (with multiple Gauss-Lobatto integration points along the beam axis) modeled using the 1D J_2 plasticity model, it can be shown that, under elastic unloading in quasistatic condition, there is an exact counteracting effect. But in general, in a complex inelastic multiple degrees-of-freedom (MDOF) system subjected to static or dynamic loading, in which we could have simultaneously elastoplastic loading and elastic unloading at different locations in the structure (due to internal stress redistribution), a general statement on the counteracting effect at elastic unloading events cannot be made. From finite-element response sensitivity analysis results for quasi-static application examples not presented here, it was also observed that some yielding events (material state transitions from elastic to plastic state) produce negligible (not visually observable) discontinuities in the nodal displacement response sensitivities. This could be due to either a smearing effect from the local to the global level or a counteracting effect between the discontinuities in the internal resisting force vector and in the consistent tangent stiffness matrix.

Ten Members Truss Subjected to Ground Motion Excitation

A ten-member truss is chosen as an example to illustrate the application of the consistent direct differentiation method (Method II) to multiple degree-of-freedom (MDOF) inelastic systems. This truss structure is subjected to the 1940 N-S component of the El Centro ground motion record (Imperial Valley Earthquake) shown in Fig. 9. The material of the truss members is modeled using the 1D J_2 (von Mises) plasticity model considered above. The geometry and material parameters (assumed common to all truss members) of the truss are given in Fig. 10. The truss structure is assumed to have mass proportional damping with a damping ratio of 5% in the first mode and decreasing as the inverse of the frequency for the higher modes. A constant time step of $\Delta t = 0.01$ s is used to integrate the equations of motion by means of the constant average acceleration Newmark-β method. The value

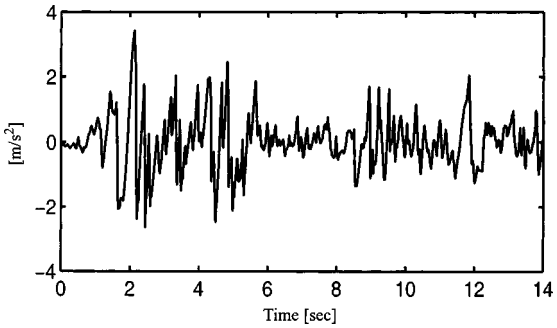

Fig. 9. Imperial valley earthquake, May 18, 1940, El Centro site, component S00E (N-S)

of the ground acceleration at every 0.02 s, starting from time $t=0$, defines the vector of loading variables $\mathbf{x}=[x_1,x_2,\ldots,x_n]^T$.

The horizontal relative displacement response history of Node 2, $u_2(t)$, is plotted in Fig. 11(a). The stress-strain hysteretic response of truss Element 1 is given in Fig. 11(b). The sensitivities of the response history $u_2(t)$ to the material Young's modulus E and initial yield stress σ_{y_0} are shown in Figs. 12 and 13, respectively. In each figure, the response sensitivity computed using the consistent DDM (Method II) is given in solid line, while response sensitivity obtained using forward finite difference analysis with decreasing values of the parameter variation is given in dashed, dashed-dot, and dotted lines. To illustrate response sensitivity analysis with respect to loading variables, Fig. 14 shows the sensitivity of $u_2(t)$ to loading parameter x_{125} [value of the ground acceleration at time $t=(125-1)\times 0.02=2.48$ s] obtained using the consistent DDM and forward finite difference analysis. As expected, loading parameter x_{125} does not influence the response until time $t=2.48$ s, and hence the response sensitivity is zero up to this time. In Figs. 12, 13, and 14, it is verified that the finite difference results converge asymptotically to those obtained using the consistent DDM, thus validating the present implementation of the DDM in *FEAP*.

Conclusions

This paper formalizes the approach (referred to herein as Method II or consistent direct differentiation method) to compute the exact (or consistent) sensitivity of the computed structural response to both material and loading parameters. This formalism

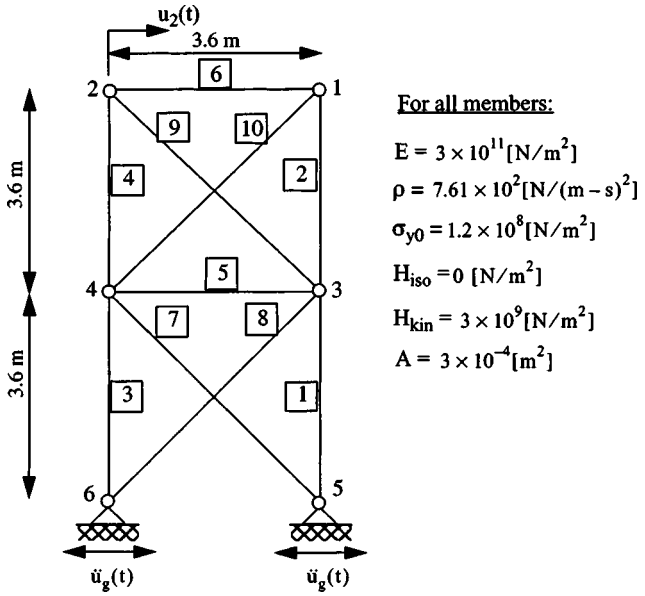

Fig. 10. Ten-member column truss structure

covers general finite-element implementations for the response prediction of a plasticity-based model of a structural system subjected to static or dynamic (e.g., earthquake) loading. The exact sensitivity of any computed structural response quantity (local or global, kinematic or static) can be obtained using this approach. Here, focus is placed on materially nonlinear-only analysis using classical plasticity theory (which assumes a yield surface within which the material is linear elastic) and the displacement-based finite-element methodology. The response sensitivities of such materially nonlinear systems exhibit discontinuities in time. It is shown that calculation of the consistent response sensitivity requires the use, at least in the last iteration of each load or time step before convergence is achieved, of the consistent (or algorithmic) material tangent moduli at the Gauss point level, which give rise to the consistent tangent stiffness matrix at the structure level. These consistent tangent moduli are used extensively in computational plasticity; they arise from consistent linearization of the numerical scheme (here return map algorithm) used to integrate the material rate constitutive equations and may differ significantly from the continuum tangent moduli for finite incremental displacements. Conditions of equivalence between the two fundamental approaches of computing the response sensitivity of

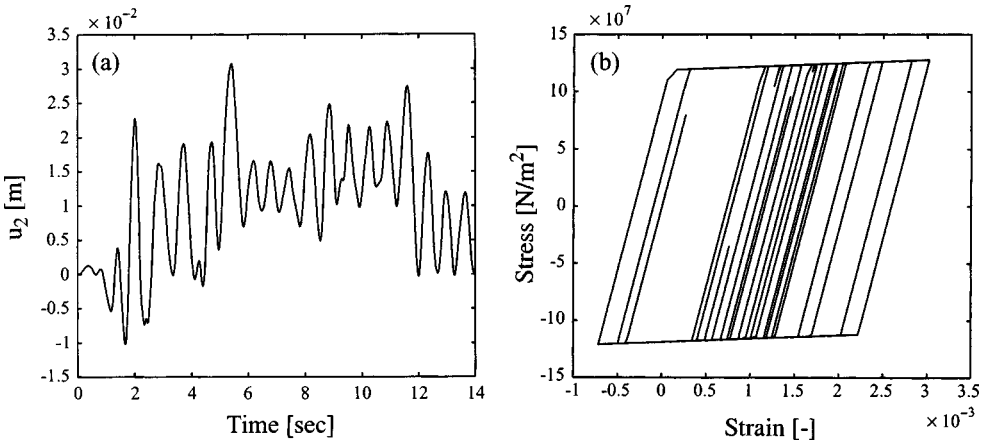

Fig. 11. (a) Horizontal relative displacement of Node 2 of ten-member truss and (b) stress-strain history of Element 1

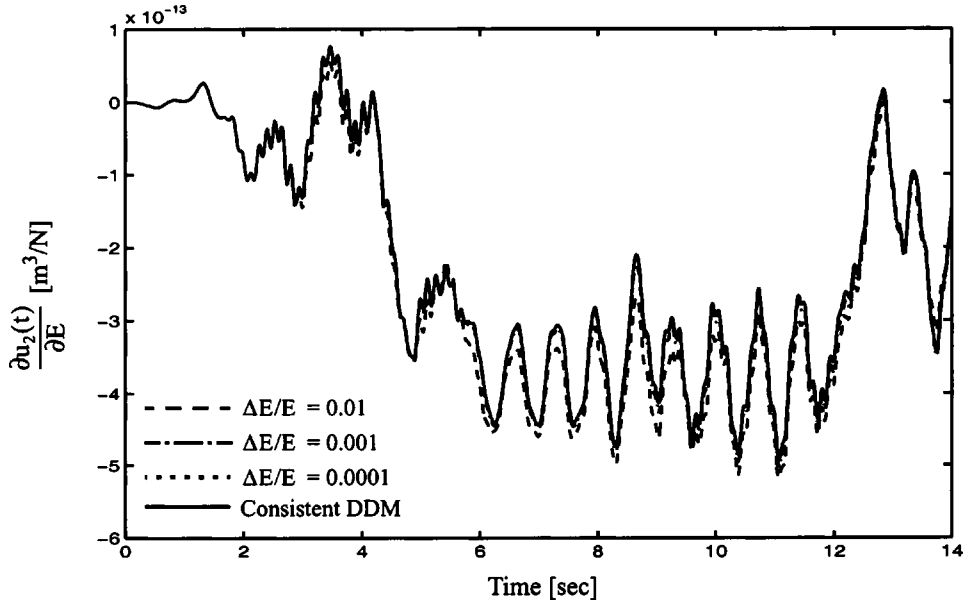

Fig. 12. Displacement response sensitivity to material Young's modulus E

inelastic (i.e., history or path dependent) dynamic systems, namely (Method I) numerical time integration of the exact semi-discretized (time continuous-spatially discrete) response sensitivity equations and (Method II) exact differentiation of the numerical finite element response algorithm (i.e., time discrete-spatially discrete response equations), have been established.

Insight is given into the nature of the discontinuities in time of response sensitivities for plasticity-based models of structural systems and their physical interpretation in terms of material state transitions through the basic 1D J_2 (von Mises) material plasticity model and two application examples. It is shown that these discontinuities are consistently carried across material state transitions through the exact differentiation of the time stepping scheme used to integrate the semi-discretized equations of motion and the numerical algorithm used to integrate the material rate constitutive equations.

Beside their intrinsic value in providing insight into system response, sensitivities of the numerically simulated response of a system to material and loading parameters represent an essential ingredient for gradient-based optimization methods needed in structural reliability analysis, structural optimization, structural identification, finite-element model updating, and structural health monitoring. The method for consistent finite-element response sensitivity analysis presented here for materially nonlinear-only dynamic structural systems can of course be used directly for nonlinear static analysis problems (by just ignoring the inertia and damping effects) and can be extended to nonlinear geometric and material models of structural systems. Although not emphasized in this paper, computing analytical finite element response sensitivities has two main advantages: (1) computational efficiency as compared to finite difference methods for estimating sensitivities, especially when dealing with a large number of sensitivity parameters as in finite element reliability analysis, and (2) overcoming the step size dilemma (Gu and Conte 2003). Regarding the latter,

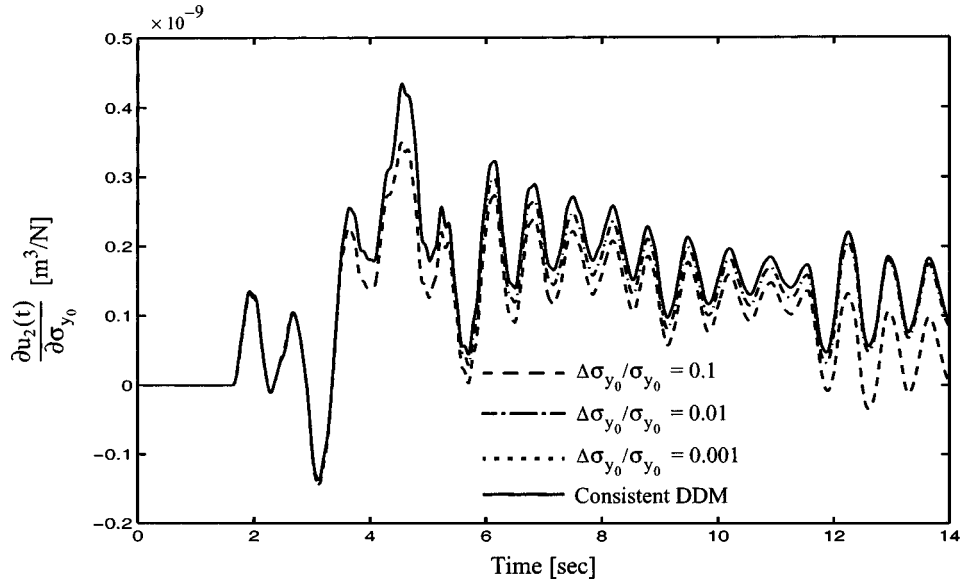

Fig. 13. Displacement response sensitivity to material initial yield stress σ_{y0}

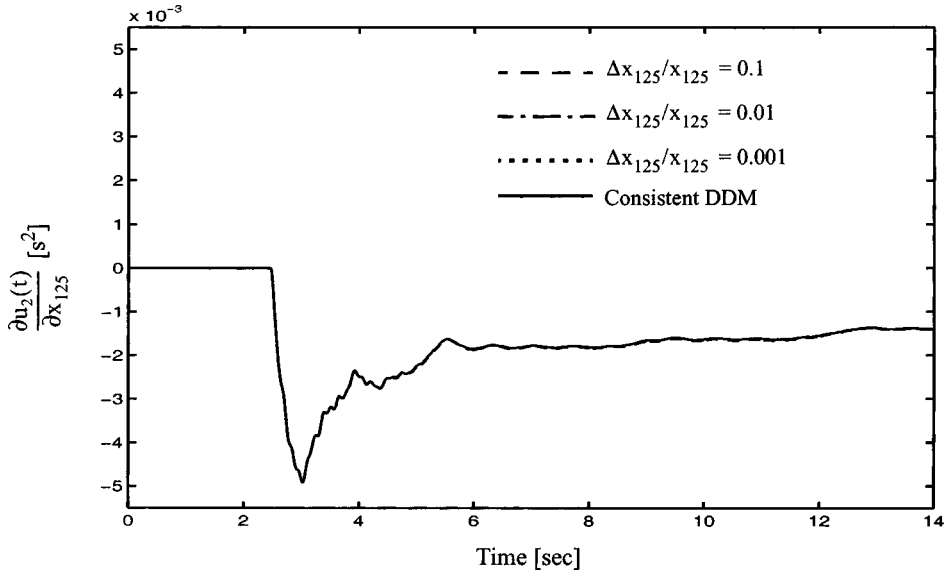

Fig. 14. Displacement response sensitivity to loading variable x_{125}

if we select the perturbation (or step size) of the sensitivity parameter to be small so as to reduce the truncation error in estimating a response sensitivity through finite difference, we may have an excessive condition error. In some cases, there may not be any step size which yields an acceptable error (Haftka and Gürdal 1992).

Acknowledgments

Support for this research by the main Italian Electricity Company (Enel—R&D Department—Centro di Ricerca Idraulica e Strutturale) is gratefully acknowledged.

References

Arora, J. S., and Cardoso, J. B. (1989). ''A design sensitivity analysis principle and its implementation into ADINA.'' *Comput. Struct.*, 32, 691–705.

Choi, K. K., and Santos, J. L. T. (1987). ''Design sensitivity analysis of non-linear structural systems. Part 1: Theory.'' *Int. J. Numer. Methods Eng.*, 24, 2039–2055.

Chopra, A. K. (2001). *Dynamics of structures: Theory and applications to earthquake engineering*, 2nd Ed., Prentice-Hall, Englewood Cliffs, N.J.

Conte, J. P. (2001). ''Finite element response sensitivity analysis in earthquake engineering.'' *Earthquake engineering frontiers in the new millennium*, Spencer and Hu, eds., Swets and Zeitlinger, Lisse, The Netherlands, 395–401.

Conte, J. P., and Jagannath, M. K. (1995). ''Seismic reliability analysis of concrete gravity dams.'' *A Report on Research Sponsored by the Main Italian Electricity Company (ENEL)*, Dept. of Civil Engineering, Rice Univ., Houston.

Conte, J. P., Jagannath, M. K., and Meghella, M. (1995). ''Earthquake response sensitivity analysis of concrete gravity dams.'' *Proc., 7th Int. Conf. on Applications of Statistics and Probability in Civil Engineering*, Paris, July 10–13, M. Lemaire, J.-L. Favre, and A. Mebarki, eds., Balkema, Rotterdam, The Netherlands, 395–402.

Conte, J. P., and Vijalapura, P. K. (1998). ''Seismic safety analysis of concrete gravity dams accounting for both system uncertainty and excitation stochasticity.'' *A Report on Research Sponsored by the Italian National Power Board (ENEL-CRIS)*, Dept. of Civil Engineering, Rice Univ., Houston.

Courant, R. (1988). *Differential and integral calculus*, Vol. II, Wiley, New York.

Ditlevsen, O., and Madsen, H. O. (1996). *Structural reliability methods*, Wiley, New York.

Gu, Q., and Conte, J. P. (2003). ''Convergence studies in nonlinear finite element response sensitivity analysis.'' *Proc. 9th Int. Conf. on Applications of Statistics and Probability in Civil Engineering*, San Francisco, July 6–9, A. Der Kiureghian, S. Madanat, and J. M. Pestana, eds., Millpress, Rotterdam, The Netherlands.

Haftka, R. T., and Gürdal, Z. (1992). *Elements of structural optimization*, Kluwer Academic, Dordrecht, The Netherlands.

Heinkenschloss, M. (1997). ''Optimization methods for optimal control problems.'' *Lecture Notes*, Summer School in Continuous Optimization, Technical Univ. Hamburg-Harburg, Germany, September.

Kleiber, M., Antunez, H., Hien, T. D., and Kowalczyk, P. (1997). *Parameter sensitivity in nonlinear mechanics: Theory and finite element computations*, Wiley, New York.

Lubliner, J. (1990). *Plasticity theory*, Macmillan, London.

Miller, A. K., ed. (1987). *Unified constitutive equations for creep and plasticity*. Elsevier Applied Science, London.

Simo, J. C., and Hughes, T. J. R. (1998). *Computational inelasticity*, Springer, Berlin.

Taylor, R. L. (1998). *FEAP—A finite element analysis program—Version 7.1 User Manual*, Dept. of Civil and Environmental Engineering, Univ. of California at Berkeley, Berkeley, Calif., 94720-1710, ⟨http://www.ce.berkeley.edu/~rlt/feap/⟩ (November 1998).

Tsay, J. J., and Arora, J. S. (1990). ''Nonlinear structural design sensitivity analysis for path dependent problems. Part 1: General theory.'' *Comput. Methods Appl. Mech. Eng.*, 81, 183–208.

Tsay, J. J., Cardoso, J. E. B., and Arora, J. S. (1990). ''Nonlinear structural design sensitivity analysis for path dependent problems. Part 2: Analytical examples.'' *Comput. Methods Appl. Mech. Eng.*, 81, 209–228.

Vijalapura, P. K., Conte, J. P., and Meghella, M. (1999). ''Time-variant reliability analysis of hysteretic SDOF systems with uncertain parameters and subjected to stochastic loading.'' *Proc., 8th Int. Conf. on Applications of Statistics and Probability in Civil Engineering*, Sydney, Australia, December 12–15, R. E. Melchers and M. G. Stewart, eds., Balkema, Rotterdam, The Netherlands, 827–834.

Zhang, Y., and Der Kiureghian, A. (1993). ''Dynamic response sensitivity of inelastic structures.'' *Comput. Methods Appl. Mech. Eng.*, 108, 23–36.

Zienkiewicz, O. C., and Taylor, R. L. (2000). *The finite element method, Vol. 2—Solid mechanics*. 5th Ed., Butterworth Heinemann, Oxford, U.K.